Article

Principle and Mechanism of Direct Porphyrin Metalation: Joint Experimental and Theoretical Investigation

Tatyana E. Shubina, Hubertus Marbach, Ken Flechtner, Andreas Kretschmann, Norbert Jux, Florian Buchner, Hans-Peter Steinrck, Timothy Clark, and J. Michael Gottfried

J. Am. Chem. Soc., **2007**, 129 (30), 9476-9483• DOI: 10.1021/ja072360t • Publication Date (Web): 11 July 2007

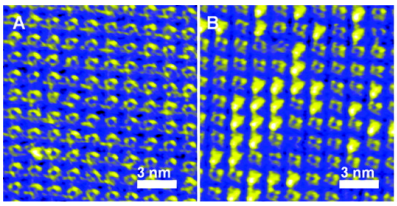

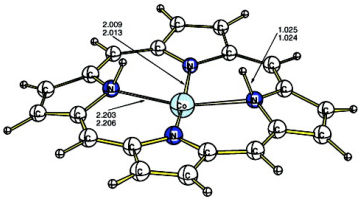

More About This Article

Additional resources and features associated with this article are available within the HTML version:

- Supporting Information
- Links to the 6 articles that cite this article, as of the time of this article download
- Access to high resolution figures
- Links to articles and content related to this article
- Copyright permission to reproduce figures and/or text from this article

View the Full Text HTML

J|A|C|S
ARTICLES
Published on Web 07/11/2007

Principle and Mechanism of Direct Porphyrin Metalation: Joint Experimental and Theoretical Investigation

Tatyana E. Shubina,*,† Hubertus Marbach,‡ Ken Flechtner,‡ Andreas Kretschmann,‡ Norbert Jux,§ Florian Buchner,‡ Hans-Peter Steinrück,‡ Timothy Clark,*,† and J. Michael Gottfried*,‡

Contribution from the Computer-Chemie-Centrum, Universität Erlangen-Nürnberg, Nägelsbachstrasse 25, 91052 Erlangen, Lehrstuhl für Physikalische Chemie II, Universität Erlangen-Nürnberg, Egerlandstrasse 3, 91058 Erlangen, and Institut für Organische Chemie II, Universität Erlangen-Nürnberg, Henkestrasse 42, 91054 Erlangen, Germany

Received April 4, 2007; E-mail: michael.gottfried@chemie.uni-erlangen.de

Abstract: The direct metalation of tetraphenylporphyrin with bare metal atoms (Co and Zn) was studied with X-ray photoelectron spectroscopy, scanning tunneling microscopy, and temperature-programmed reaction measurements on ordered monolayer films of the molecules adsorbed on a Ag(111) surface. The mechanism of this novel type of surface reaction was investigated using density functional theory (DFT) calculations for the related gas-phase reactions of the unsubstituted porphyrin with the metals Fe, Co, Ni, Cu, and Zn. The reaction starts with the formation of an initial complex, in which the metal atom is coordinated by the intact unreduced porphyrin. This complex resembles the sitting-atop complex proposed for porphyrin metalation with metal ions in solution. In two subsequent steps, the pyrrolic hydrogen atoms are transferred to the metal atom, forming H_2, which is eventually released. The activation barriers of the H-transfer steps vary for the different metal atoms. DFT calculations suggest that metalations with Fe, Co, and Ni show two-state reactivity, while those with Cu and Zn proceed on a single potential energy surface. For metalation with Zn, we calculated a barrier of the first hydrogen transfer step of 32.6 kcal mol^{-1}, in good agreement with the overall experimental activation energy of 31 kcal mol^{-1}.

Introduction

Metalloporphyrins were formed early in the history of the prebiotic earth and played an important role in, for instance, catalyzing the disproportionation of hydrogen peroxide.[1,2] Naturally occurring metalloporphyrins are among the most important prosthetic groups for oxygen storage and transfer,[3] metabolism,[4,5] photosynthesis,[6] and many other redox reactions and small-molecule storage and transport purposes in biological systems. Synthetic porphyrins have been used extensively as model systems for investigating the complex biological functions of natural porphyrin-containing systems. Although seemingly far removed from these important biological systems, ordered monolayers of porphyrins on inert surfaces[7−16] offer a unique opportunity to study the reactivity of porphyrin systems without the perturbing influences of solvation, counterions, the protein environment, an oxidizing atmosphere, or other environmental effects. Generally, the influence of the surface on which the porphyrins are adsorbed is considerably better defined (especially in the case of a single-crystal surface) than most other environmental effects found in condensed-phase systems. In addition, metalloporphyrins are particularly suitable for surface functionalization on the nanoscale, which is the key to tailoring sensors, catalysts, and other devices whose functional principle is based on the interaction of an active solid surface with another (liquid or gaseous) phase. They combine a structure-forming element, the porphyrin framework, with an active site, the coordinated metal ion. Another particular advantage of these thin-film systems is that reactions such as coordination of metal

† Computer-Chemie-Centrum.
‡ Lehrstuhl für Physikalische Chemie II.
§ Institut für Organische Chemie II.

(1) Hodgson, G. W.; Ponnamperuna, C. *Proc. Natl. Acad. Sci. U.S.A.* **1968**, *59*, 22.
(2) Kamaluddin, M. S.; Singh, M.; Deopujari, S. W. *Origins Life Evol. Biospheres* **2005**, *17*, 59.
(3) Chapman, S. K.; Daff, S.; Munro, A. W. *Struct. Bonding* **1997**, *88*, 39.
(4) *Metabolic Pathways*; Greenwoord, D. M., Ed.; Academic Press: New York, 1969; Vol. 3: Amino Acids and Tetrapyrroles.
(5) Lewis, D. F. V. *Cytochromes P450: Structure, Function and Mechanism*; Taylor and Francis: London, 1996.
(6) *Tetrapyrrole Photoreceptors in Photosynthetic Organisms*; Beale, S. I., Ed.; Kluwer Academic Publishers: Dordrecht, Netherlands, 2002; Vol. 74(2), p 138.
(7) Barlow, D. E.; Scudiero, L.; Hipps, K. W. *Langmuir* **2004**, *20*, 4413.
(8) Williams, F. J.; Vaughan, O. P. H.; Knox, K. J.; Bampos, N.; Lambert, R. M. *Chem. Commun.* **2004**, 1688.
(9) Vaughan, O. P. H.; Turner, M.; Williams, F. J.; Hille, A.; Sanders, J. K. M.; Lambert, R. M. *J. Am. Chem. Soc.* **2006**, *128*, 9578.
(10) Vaughan, O. P. H.; Williams, F. J.; Bampos, N.; Lambert, R. M. *Angew. Chem., Int. Ed.* **2006**, *45*, 3779.
(11) Katsonis, N.; Vicario, J.; Kudernac, T.; Visser, J.; Pollard, M. M.; Feringa, B. L. *J. Am. Chem. Soc.* **2006**, *128*, 15537.
(12) Gottfried, J. M.; Flechtner, K.; Kretschmann, A.; Lukasczyk, T.; Steinrück, H.-P. *J. Am. Chem. Soc.* **2006**, *128*, 5644.
(13) Buchner, F.; Schwald, V.; Comanici, K.; Steinrück, H.-P.; Marbach, H. *ChemPhysChem* **2007**, *8*, *241*.
(14) Auwärter, W.; Weber-Bargioni, A.; Brink, S.; Riemann, A.; Schiffrin, A.; Ruben, M.; Barth, J. V. *ChemPhysChem* **2007**, *8*, *250*.
(15) Kretschmann, A.; Walz, M.-M.; Flechtner, K.; Steinrück, H.-P.; Gottfried, J. M. *Chem. Commun.* **2007**, 568.
(16) Lukasczyk, T.; Flechtner, K.; Merte, L. R.; Jux, N.; Maier, F.; Gottfried, J. M.; Steinrück, H.-P. *J. Phys. Chem. C* **2007**, *111*, 3090.

10.1021/ja072360t CCC: $37.00

atoms[11−15] or attachment of ligands[8] can be studied with surface-science techniques. These techniques, such as, for example, photoelectron spectroscopy or scanning tunneling spectroscopy (STM), use ultra-high-vacuum (UHV) conditions, which ensure the absence of the environmental effects outlined above. The high thermal stability of many (metallo)porphyrins allows for film preparation by evaporation deposition despite the high molecular weight of the molecules.[17] Alternatively, ordered monolayers films of metalloporphyrins can be obtained by the direct metalation of porphyrins adsorbed on an inert metal surface by bare transition-metal atoms under UHV conditions.[12−14] This approach allows the in situ synthesis of those metalloporphyrins that are too reactive to be synthesized in solution or not thermally stable enough for evaporation deposition.

We recently reported the first examples of the formation of cobalt(II) and iron(II) tetraphenylporphyrins (MTPPs, M = Co, Fe)[12,13] from the direct reaction of the bare metal atoms (Co or Fe) and adsorbed tetraphenylporphyrin (2HTPP) molecules. Until now, we[12,13,15] and others[14] were only able to speculate about the reaction mechanism, since the reaction is fast at 300 K (on the time scale of our experiment, i.e., several minutes) and no intermediates could be observed. Lowering the temperature to reduce the reaction rate is not a useful option because this could make the diffusion of the metal atoms rate limiting. Therefore, we needed to find a metal for which the activation barrier of the metalation reaction is sufficiently high to make the reaction slow at 300 K. Zinc proved to fulfill this condition.[15]

The wealth of mechanistic pathways open to transition metals suggests such direct metalation reactions to be interesting candidates for mechanistic studies. Although several theoretical studies of porphyrin metalation by divalent metal ions in solution have been reported,[18−20] we are not aware of any theoretical studies of the corresponding reaction with bare metal atoms. There have, however, been many previous studies of the electronic structures of the metalloporphyrins.[21−26] These have revealed states of different spin multiplicities that are close in energy in many cases and, of particular interest for this study, the possibility of two-state reactivity (TSR)[27] in porphyrin reactions. This concept has been used successfully to explain reactivity patterns in biological systems, usually containing iron−oxo species, and gas-phase chemistry of transition-metal ions.[28] A prerequisite for TSR is usually a high-spin ground state of the reactant and a low-lying low-spin excited state. Since the products of the direct metalation reaction have spin states different from those of the reactants, one would expect spin crossover to occur in the course of the reaction. However, to the best of our knowledge, there are no studies involving reactions with porphyrins that show the possibility of TSR without axial ligands. Thus, experimental studies of relatively unperturbed reactions of porphyrins adsorbed on inert metal surfaces combined with theoretical investigations of the same reactions in vacuo promise to provide a wealth of new information about this important class of compounds. We therefore now report a combined experimental and theoretical study of this unusual reaction under well-defined conditions.

In the following, we report a detailed analysis of direct experimental observations of the metalation reaction for Co and Zn and gas-phase density functional theory (DFT) calculations of the reaction pathways for Co, Fe, Ni, Cu, and Zn atoms with porphyrin (2HP), which has been used as a model for 2HTTP.

Methods

Experimental Techniques. The X-ray photoelectron spectroscopy (XPS) experiments were performed with a Scienta ESCA-200 spectrometer equipped with an Al Kα X-ray source (1486.6 eV), a monochromator, and a hemispherical energy analyzer (SES-200). The overall energy resolution amounts to 0.3 eV. The binding energies are referenced to the Fermi edge of the clean Ag surface ($E_B \equiv 0$). The STM images were acquired in a second UHV system using an RHK UHV VT STM 300 with SPM 100 electronics and cut Pt/Ir tips as STM probes. The images were taken in constant-current mode. Voltages are given with respect to the sample. Moderate low-pass filtering was applied for noise reduction. The STM data were processed with WSxM.[29] The base pressure in both UHV systems is in the low 10^{-10} mbar regime. The coverage θ is defined as the number of adsorbed molecules or atoms divided by the number of substrate atoms; "monolayer" denotes a closed adlayer of molecules with direct contact to the substrate surface. Monolayers of 2HTPP and all MTPPs investigated experimentally correspond to $\theta = 0.037$. This value was determined with a combination of XPS, low-energy electron diffraction, and STM. Well-ordered monolayers of all porphyrins (specified purity >98%, Porphyrin Systems) were prepared by evaporation deposition of multilayers at 300 K and subsequent annealing at 525 K as described by Lukasczyk et al.[16] N-deuterated tetraphenylporphyrin (2DTPP) was prepared by reaction of 2HTPP with diluted D_2SO_4 at ambient temperature. The degree of deuteration was determined by NMR spectroscopy and was found to be >80%. The deposition of metal atoms was achieved with an Omicron EFM 3 electron-beam evaporator (Co) or with a Knudsen cell evaporator (Zn). The sample was a Ag single crystal (purity >99.999%) with a polished (111) surface, which was aligned to <0.1° with respect to the nominal orientation.

Computational Methods. Geometries of all structures were fully optimized at the B3LYP[30−33] level of theory using the 6-31G(d)[34−44] basis set and the 6-31G(d, p) basis set in combination with the LANL2DZ[45−47] basis set with pseudopotentials for Co, Fe, Ni, Cu, and

(17) Scudiero, L.; Barlow, D. E.; Mazur, E.; Hipps, K. W. *J. Am. Chem. Soc.* **2001**, *123*, 4073.
(18) Shen, Y.; Ryde, U. *J. Inorg. Biochem.* **2004**, *98*, 878.
(19) Shen, Y.; Ryde, U. *Chem.—Eur. J.* **2005**, *11*, 1549.
(20) Hsiao, Y. W.; Ryde, U. *Inorg. Chim. Acta.* **2006**, *359*, 1081.
(21) Choe, Y.-K.; Nakajima, T.; Hirao, K.; Lindh, R. *J. Chem. Phys.* **1999**, *111*, 3837.
(22) Liao, M.-S.; Watts, J. D.; Huang, M.-J. *J. Phys. Chem. A* **2005**, *109*, 7988.
(23) Liao, M.-S.; Scheiner, S. *J. Chem. Phys.* **2002**, *117*, 205.
(24) Liao, M.-S.; Scheiner, S. *J. Comput. Chem.* **2002**, *23*, 1391.
(25) Kozlowski, P. M.; Spiro, T. G.; Berces, A.; Zgierski, M. Z. *J. Phys. Chem. B* **1998**, *102*, 2603.
(26) Rovira, C.; Kunc, K.; Hutter, J.; Parrinello, M. *Inorg. Chem.* **2001**, *40*, 11.
(27) Schroeder, D.; Shaik, S.; Schwarz, H. *Acc. Chem. Res.* **2000**, *33*, 139.
(28) Shaik, S.; Danovich, D.; Fiedler, A.; Schroeder, D.; Schwarz, H. *Helv. Chim. Acta* **1975**, *78*, 1393.
(29) WSxM, http://www.nanotec.es.
(30) Becke, A. D. In *The Challenge of d- and f-electrons: Theory and Computation*; Salahub, D. R., Zerner, M. C., Eds.; American Chemical Society: Washington, DC, 1989; Chapter 12, p 165.
(31) Vosko, S. H.; Wilk, L.; Nusair, M. *Can. J. Phys.* **1980**, *58*, 1200.
(32) Lee, C.; Yang, W.; Parr, R. G. *Phys. Rev. B* **1988**, *37*, 785.
(33) Becke, A. D. *J. Chem. Phys.* **1993**, *98*, 5648.
(34) Ditchfield, R.; Hehre, W. J.; Pople, J. A. *J. Chem. Phys.* **1971**, *54*, 724.
(35) Hariharan, P. C.; Pople, J. A. *Theor. Chim. Acta* **1973**, *28*, 213.
(36) Hariharan, P. C.; Pople, J. A. *Mol. Phys.* **1974**, *27*, 209.
(37) Hehre, W. J.; Ditchfield, R.; Pople, J. A. *J. Chem. Phys.* **1972**, *56*, 2257.
(38) Gordon, M. S. *Chem. Phys. Lett.* **1980**, *76*, 163.
(39) Blaudeau, J.-P.; McGrath, M. P.; Curtiss, L. A.; Radom, L. *J. Chem. Phys.* **1997**, *107*, 5016.
(40) Francl, M. M.; Pietro, W. J.; Hehre, W. J.; Binkley, J. S.; DeFrees, D. J.; Pople, J. A.; Gordon, M. S. *J. Chem. Phys.* **1982**, *77*, 3654.
(41) Binning, J., R. C.; Curtiss, L. A. *J. Comput. Chem.* **1990**, *11*, 1206.
(42) Rassolov, V. A.; Pople, J. A.; Ratner, M. A.; Windus, T. L. *J. Chem. Phys.* **1998**, *109*, 1223.
(43) Rassolov, V. A.; Ratner, M. A.; Pople, J. A.; Redfern, P. C.; Curtiss, L. A. *J. Comput. Chem.* **2001**, *22*, 976.
(44) Frisch, M. J.; Pople, J. A.; Binkley, J. S. *J. Chem. Phys.* **1984**, *80*, 3265.
(45) Wadt, W. R.; Hay, P. J. *J. Chem. Phys.* **1985**, *82*, 284.
(46) Hay, P. J.; Wadt, W. R. *J. Chem. Phys.* **1985**, *82*, 270.
(47) Hay, P. J.; Wadt, W. R. *J. Chem. Phys.* **1985**, *82*, 299.

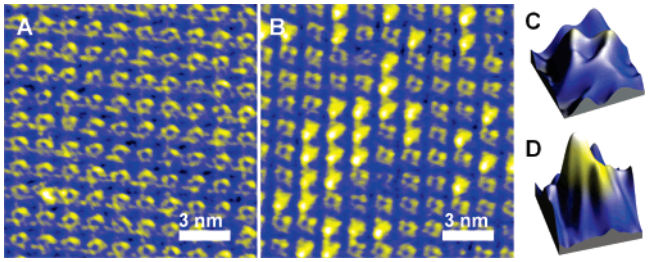

Figure 1. Room-temperature constant-current STM images of a monolayer of 2HTPP (A) and after the evaporation of Co, $\theta_{Co} = 0.012 \pm 0.002$ (B). Both images were acquired at a current set point of 30 pA and bias voltages of −0.15 and −0.21 V in (A) and (B), respectively. The 3D plots in (C) and (D) are extracted from single molecules in (B) and represent a single 2HTPP and CoTPP molecule, respectively. The height ranges are (C) 0−0.0062 nm and (D) 0−0.011 nm.

Zn atoms. This combination is denoted B3LYP/6-31G(d,p)+LANL2DZ) in the following. The Gaussian 03 program package was used for all calculations.[48] Structures that contained Co, Ni, and Fe atoms were also optimized at the B3LYP*/6-31G(d) level of theory.[49] We used different levels of theory because it is not clear[50] which combination of density functional method and basis sets is more appropriate for treating metalloporphyrin systems. Stationary points were confirmed to be minima or transition states by calculating the normal vibrations within the harmonic approximation. All relative energies are corrected for zero-point vibrational energies (ZPVEs).

Results and Discussion

Scanning Tunneling Microscopy. As previously shown, the reaction of adsorbed tetraphenylporphyrin with bare cobalt[12] and iron[13,14] atoms is fast at 300 K. Therefore, if activation barriers exist, they must be lower than ∼20 kcal mol^{-1}. In contrast, metalation with Zn is very slow at 300 K and requires heating to ∼550 K.[15]

To extend and strengthen these experimental findings and to illustrate the coordination of Co atoms with 2HTPP, we now report the first microscopic evidence for this in situ metalation reaction with Co. These results were obtained using the procedure described in ref 13. Figure 1A shows a high-resolution STM image of a monolayer of 2HTPP. The molecules lie flat on the surface and are ordered in a square arrangement with a lattice constant of 1.4 nm. The central porphyrin rings are clearly visible, and the centers of the molecules appear as depressions (see also Figure 1C). After the evaporation deposition of cobalt ($\theta_{Co} = 0.012 \pm 0.002$, i.e., one-third of the stoichiometric amount required for the complete metalation of the 2HTPP monolayer), the STM image shown in Figure 1B was obtained. About 31% (statistics over larger scan areas) of the molecules now appear as protrusions (see also Figure 1D) that can be identified as CoTPP,[51] whereas the remainder still exhibit the features associated with 2HTPP. This indicates a high efficiency, close to 100%, for the Co metalation at the given amount of evaporated Co, which is similar to our findings for Fe.[13] These results together with our earlier spectroscopic findings[12] provide clear evidence for the Co metalation and some details associated with the process. However, the limitations of the experimental setup do not allow for the observation of the individual steps involved in the complexation process itself, e.g., due to the instrumental time resolution. Thus, it is now important to develop a theoretical understanding of the mechanism of the metalation reaction.

Density Functional Theory Calculations. The question arises as to whether the metalation is a one-step reaction or whether one or more intermediate species exist. The complexity of the reaction (insertion of the metal atom (M), oxidation to M^{2+} and parallel reduction of hydrogen, release of H_2) makes a multistep reaction probable. Even for porphyrin metalation in solution, where usually no redox reaction involving dihydrogen is observed, an intermediate has been proposed.[52] In this "sitting-atop" (SAT) complex, the metal ion is already coordinated to the nitrogen atoms of the porphyrin while the pyrrolic hydrogen atoms are still in place.[20]

To obtain insight into possible reaction mechanisms, we performed DFT calculations of the reaction of Co and other transition-metal atoms with the porphyrin molecule (2HP). Figure 2 shows the lowest energy reaction profile for the reaction of a bare Co atom with 2HP at the different levels of theory. The first stage of the reaction is the barrierless formation of the novel 2*H*-metalloporphyrin complex **1** (denoted the *initial complex* in the following). This reaction is found to be exothermic with respect to the Co atom and 2HP at infinite separation by −46.3 and −52.3 kcal mol^{-1} at the B3LYP/6-31G(d,p)+LANL2DZ level for the high-spin (HS, spin 3/2) and low-spin (LS, spin 1/2) states, respectively (energy differences with respect to the low-spin complex **1**). At two other levels of theory {B3LYP/6-31G(d) and B3LYP*/6-31G(d)} reaction is even more exothermic. However, the separation between the ^{4}Co and ^{2}Co states becomes somewhat too large (up to 40 kcal mol^{-1}, Figure 2). The quartet HS and doublet LS states, ^{4}**1** and ^{2}**1**, have similar geometries with a distorted porphyrin core and differ in energy by only 0.1 kcal mol^{-1} at both the B3LYP/6-31G(d,p)+LANL2DZ and B3LYP/6-31G(d) levels. At the B3LYP*/6-31G(d) level ^{2}**1** was found to be more stable than ^{4}**1** by 10.2 kcal mol^{-1}. We cannot therefore assign a ground-state multiplicity from the results of our calculations. The geometry of this initial complex **1** can be described in terms of an SAT complex (Figure 3), the formation of which has been proposed for a variety of reactions between porphyrins and metal *ions* in solution.[52]

The reaction can proceed from the initial complex **1** by two pathways. ^{2}**1** and ^{4}**1** form intermediates ^{2}**2** and ^{4}**2** via the late transition states ^{2}**TS1** and ^{4}**TS1**, which describe a hydrogen atom transfer from the nitrogen to the metal atom. We were unable to find the LS transition state ^{2}**TS1** for this rearrangement at the B3LYP/6-31G(d) level, despite many attempts. However, the computed barrier for the high-spin reaction via transition state ^{4}**TS1** was found to be 9.4 kcal mol^{-1}. The computed barriers at the B3LYP/6-31G(d, p)+LANL2DZ level are 13.2 and 15.7 kcal mol^{-1} for low and high spins, respectively (with respect to the low-spin complex **1**). The energy difference between the two transition states is 1.5 kcal mol^{-1}, with LS ^{2}**TS1** being the more stable. Similar trends in relative stability, but far lower barriers, were found at the B3LYP*/6-31G(d) level (the barrier for the rearrangement is 0.5 kcal mol^{-1} for low spin and the low-spin transition state ^{2}**TS1** is 2.6 kcal mol^{-1} more stable than ^{4}**TS1**). However, this energy difference is once more

(48) Frisch, M. J.; et al., Gaussian, Inc., Wallingford, CT, 2004.
(49) Reiher, M.; Salomon, O.; Hess, B. A. *Theor. Chem. Acc.* **2001**, *107*, 48.
(50) Liao, M.-S.; Watts, J. D.; Huang, M.-J. *J. Comput. Chem.* **2006**, *27*, 1577.
(51) Scudiero, L.; Barlow, D. E.; Hipps, K. W. *J. Phys. Chem. B* **2000**, *104*, 11899.
(52) Fleischer, E. B.; Wang, J. H. *J. Am. Chem. Soc.* **1960**, *82*, 3498.

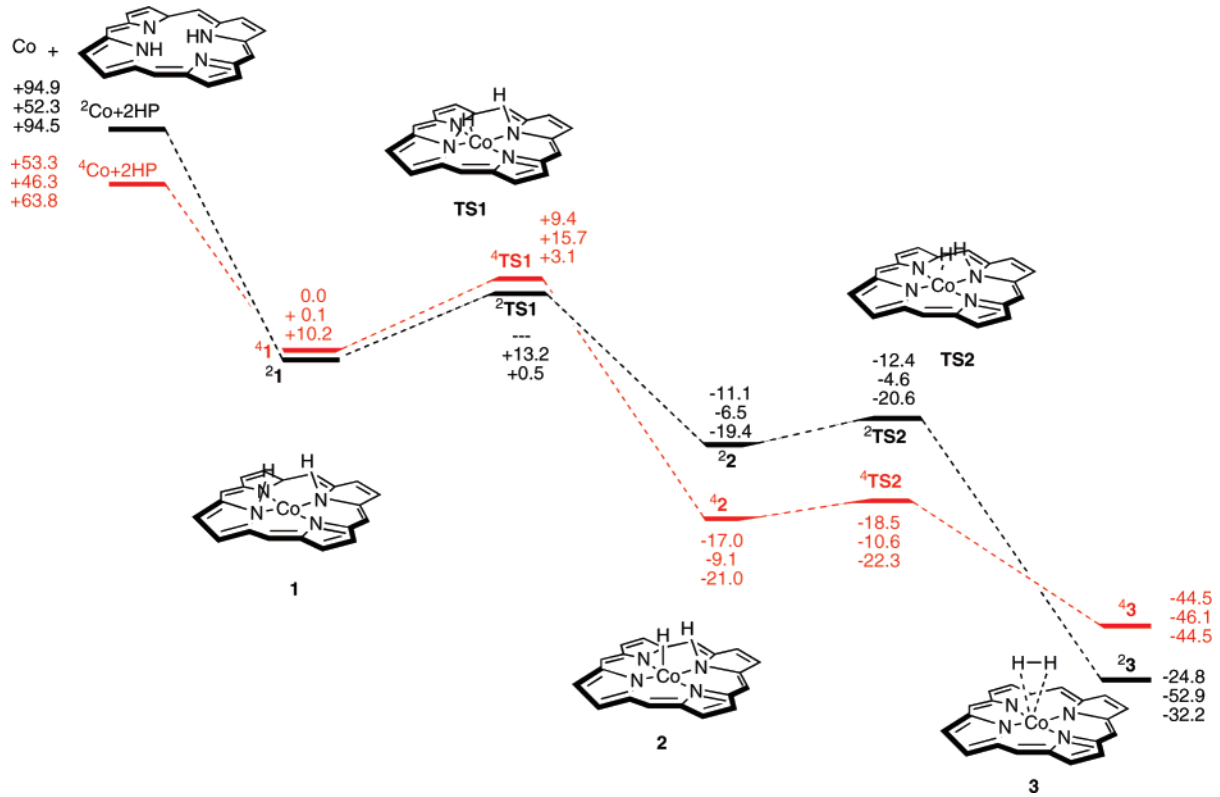

Figure 2. Schematic energy profile for Co atom insertion into 2HP {ΔE + ZPE in kcal mol^{-1} at B3LYP/6-31G(d) (first entry), B3LYP/6-31G(d,p)+LANL2DZ (second entry), and B3LYP*/6-31G(d) (third entry)}.

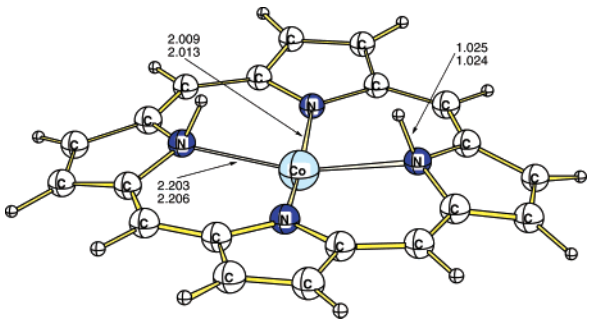

Figure 3. Optimized geometries (B3LYP/6-31G(d,p)+ECP LANL2DZ) of the initial complexes ^{2}**1** (first entry) and ^{4}**1** (second entry). Bond lengths are in angstroms.

too small for us to be able to assign a ground-state multiplicity for the transition state.

The formation of intermediate **2** is exothermic for both the HS and LS pathways. However, the computed values of ΔE depend on the choice of functional and basis sets (Figure 2). Nevertheless, the high-spin state ^{4}**2** was found to be somewhat more stable than ^{2}**2**.

The next reaction step is the very exothermic (up to 46.4 kcal mol^{-1}) formation of the CoP$\cdots$H$_2$ complex **3** via the transition state ^{4}**TS2** (high-spin pathway) or via the transition state ^{2}**TS2** (low spin). Both transition states ^{4}**TS2** and ^{2}**TS2** occur early and describe synchronous hydrogen abstraction from the pyrrolic nitrogen and formation of H$_2$. The reaction barrier for this process is calculated to be only 1.9 kcal mol^{-1} for the low-spin pathway (B3LYP/6-31G(d, p)+LANL2DZ) and is even smaller at the B3LYP/6-31G(d) and B3LYP*/6-31G(d) levels of theory (Figure 2).

The final complex **3** can be described as Co^{II}P with a loosely bound H$_2$ molecule. Thus, one would expect **3** to have properties similar to those of Co^{II}P. The results obtained at the B3LYP/631G(d,p) +LANL2DZ level predict **3** to have a doublet ground state, while calculations with B3LYP and B3LYP* functionals with the 6-31G(d) basis set predict it to be high-spin. The difference between spin states, however, is about 7 kcal mol^{-1} at the B3LYP/6-31G(d, p)+LANL2DZ level and much larger (ca. 12−20 kcal/mol) at the other two levels. Previous calculations of Co^{II}P identified the low-spin state as the ground state, and the HS state was found to be 16.9 kcal mol^{-1} above the ground state.[26]

Thus, the overall reaction starting from the high-spin state for the Co atom and ending with the formation of Co^{II}P can presumably be described as a two-state reactivity process.

The situation described above for the reaction of Co with 2HP is reproduced with some minor changes for the corresponding reactions of Fe and Ni (Figures 4 and S1 of the Supporting Information).

The reaction with Fe is somewhat more complicated as it also involves participation of an intermediate-spin (IS, $S = 1$) state between the LS ($S = 0$) and the HS ($S = 2$) states in the course of the reaction. From the initial complex **4** the reaction proceeds virtually without barriers until the final complex **6** is formed. In the case of both ^{1}**TS3** and ^{1}**TS4**, the activation energies with respect to ^{1}**4** and ^{1}**5** were found to be 2.9 and 0.5 kcal mol^{-1}, respectively, without ZPVE correction. With ZPVE applied both ^{1}**TS3** and ^{1}**TS4** become lower on the potential energy surface than the corresponding complexes ^{1}**4** and ^{1}**5** by 0.3 and 1.3 kcal mol^{-1}, respectively (at the B3LYP/6-31G(d,p)+LANL2DZ level of theory). In some cases we were

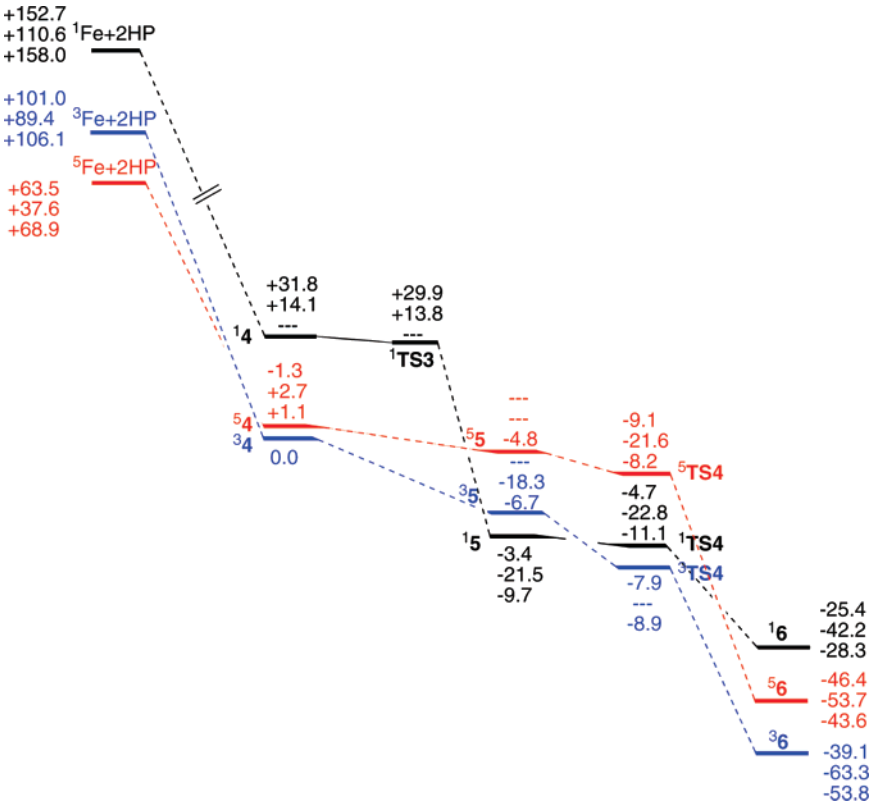

Figure 4. Energy profile for Fe atom insertion into 2HP {ΔE + ZPE in kcal mol^{-1} at B3LYP/6-31G(d) (first entry), B3LYP/6-31G(d,p)+LANL2DZ (second entry), and B3LYP*/6-31G(d) (third entry)}.

unable to locate transition states and local minima at all three levels of theory.

Again, similar to the situation with Co, the final complex **6** can be described as $Fe^{II}P\cdots H_2$. Thus, one would expect **6** to have properties similar to those of the free $Fe^{II}P$ porphyrin. Previously, extensive calculations[22,24] and experimental data[53] for FeTPP suggested that $Fe^{II}P$ has a $^3A_{2g}$ ground state and that the energy separation between the triplet and the lowest quintet $^5A_{1g}$ is 16.4 kcal mol^{-1} (the experimental value for FeTPP is 14.3 kcal mol^{-1}).[53] Both B3LYP/6-31G(d, p)+LANL2DZ and B3LYP*/6-31G(d) predict ^{3}**6** to be more stable than ^{5}**6** by ca. 10 kcal mol^{-1}, while at the B3LYP/6-31G(d) level ^{5}**6** is more stable than ^{3}**6** by 7.3 kcal mol^{-1}.

Nevertheless, the overall reaction with the Fe atom can also be described as a two-state reactivity process, in which intermediate- and high-spin states are competive in energy and may cross.

The reaction of Ni with 2HP differs from that with Co in that the formation of complex **11** via transition states ^{1}**TS7** and ^{3}**TS7** has significantly higher activation barriers (+29.2 and +28.8 kcal mol^{-1}, respectively, B3LYP/6-31G(d,p)+LANL2DZ) than those found for iron and cobalt (Figure S1 of the Supporting Information). The choice of functional and basis sets plays a crucial role. All three levels of theory used here predict a very large energy gap between ^{1}Ni and ^{3}Ni, although the results obtained at the B3LYP/6-31G(d, p)+LANL2DZ level give a more realistic picture with respect to available experimental data[54] and calculations.[55,56] It is also worth mentioning that there is virtually no separation between triplet and singlet states in **11**, which suggests that spin crossover can occur near this structure.

In contrast to these reactions with the earlier transition metals, those with Zn and Cu (Figures 5 and S2 of the Supporting Information) are calculated to proceed on single potential energy surfaces with spins 0 and 1/2 for Zn and Cu, respectively.

In the case of Zn metalation of 2HP, formation of intermediate **8** from the SAT complex **7** is associated with the activation barrier (Figure 5, +32.6 and +34.8 kcal mol^{-1}, B3LYP/6-31G(d) and B3LYP/6-31G(d,p)+LANL2DZ, respectively).

Reaction with Cu proceeds similarly to that with Zn with a lower activation energy (+23.8 kcal mol^{-1}, B3LYP/6-31G(d), Figure S2 of the Supporting Information).

The results obtained at the B3LYP/6-31G(d) level appear to be more reliable for the later transition metals (Cu and Zn) than those at the B3LYP/6-31G(d,p)+LANL2DZ level because the latter predict that the formation of the initial complex for zinc is endothermic, which disagrees with the experimental observations.

X-ray Photoelectron Spectroscopy. For the spectroscopic investigation of the metalation reaction, we used the procedure described in ref 12. Briefly, we prepared well-defined, ordered monolayers of 2HTPP on a Ag(111) surface and subsequently deposited stoichiometric amounts of the metal atoms. All preparation and analysis steps were performed in a UHV environment (see the Methods). Since this work is focused on the reaction mechanism, we concentrate here on the metalation

(53) Boyd, P. D. W.; Buckingham, D. A.; McMecking, R. F.; Mitra, S. *Inorg. Chem.* **1979**, *18*, 3585.
(54) Moore, S. E. *Atomic Energy Levels*; NSRDS: Washington, DC, 1971.
(55) Mebel, A. M.; Hwang, D.-Y. *J. Phys. Chem. A* **2000**, *104*, 11622.
(56) Li, T.; Xie, X.; Gao, S.; Wang, C.; Cheng, W.; Pan, X.; Cao, H. *J. Mol. Struct.: THEOCHEM* **2005**, *724*, 125.

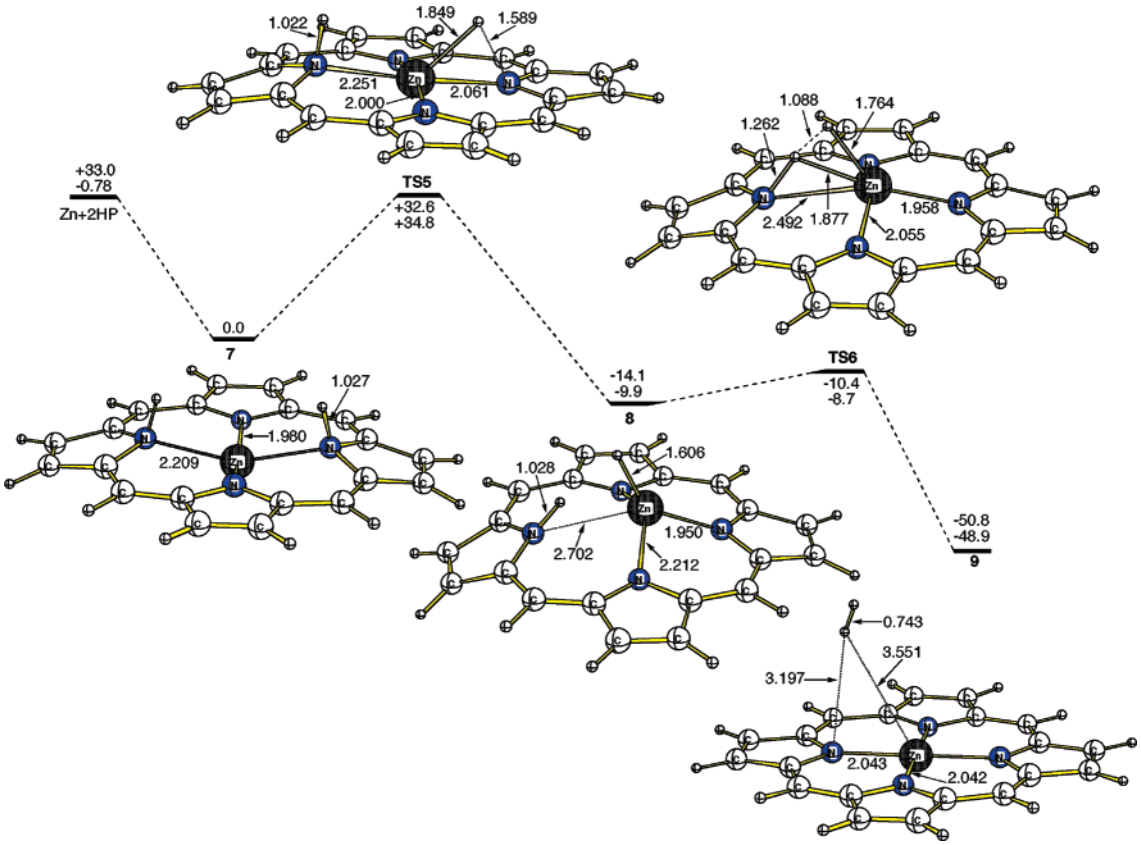

Figure 5. Schematic energy profile for Zn atom insertion into 2HP {ΔE + ZPE in kcal mol^{-1} at B3LYP/6-31G(d) (first entry) and B3LYP/6-31G-(d,p)+LANL2DZ (second entry)}. Bond lengths are in angstroms.

with zinc as the "slowest" of the reactions investigated, and thus that that can provide the most mechanistic information.

Chemical analysis of the reaction systems was performed with XPS. For studying metalation with Zn, we monitored two core-level signals, N 1s and Zn $2p_{3/2}$. In addition, we recorded C 1s spectra, which did not significantly change during metalation.

Figure 6A shows the N 1s XP spectrum of a monolayer of 2HTPP on the Ag(111) surface. The two signals are assigned to iminic (398.2 eV) and pyrrolic (400.1 eV) nitrogen atoms.[12,15,57−59] Vapor deposition of a small excess of Zn atoms ($\theta_{Zn} = 0.038$; see the Methods) on this 2HTPP monolayer results in the complex signal shown in Figure 6B. Subsequent heating to 550 K induces formation of ZnTPP (Figure 6C), as confirmed by comparison with the monolayer spectrum of directly vapor-deposited ZnTPP (Figure 6D).

The simplest possible approach to interpreting the complicated signal in Figure 6B assumes that it arises from a mixture of the product, ZnTPP, and unreacted 2HTPP. Accordingly, we attempted a deconvolution with the fitted signals of 2HTPP (blue lines) and ZnTPP (green line). However, this did not result in a satisfactory agreement between the spectrum and the fitting curve. To obtain better agreement, it was necessary to introduce two additional peaks, represented by the orange curves. These additional signal components indicate the presence of an intermediate species, in which the nitrogen atoms are not equivalent. This intermediate is probably identical to the initial

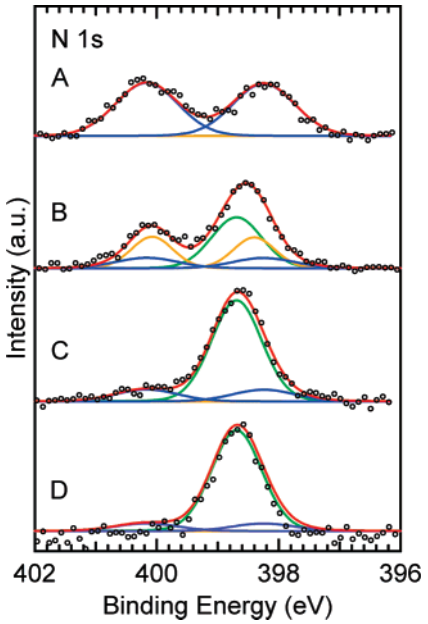

Figure 6. N 1s XPS spectra of (A) a monolayer of 2HTPP on Ag(111), (B) after vapor deposition of Zn on the 2HTPP monolayer at 300 K ($\theta_{Zn} = 0.038$), and (C) after subsequent heating of the Zn/2HTPP coadsorbate to 550 K. (D) N 1s XPS spectrum of a monolayer of ZnTPP on Ag(111) for comparison. Line colors: blue, 2HTPP; green, ZnTPP; orange, intermediate; red, envelope.

complex **7** (see Figure 5 and discussion of the computational results above), in which the Zn atom is coordinated by the porphyrin, while the two pyrrolic N−H bonds are still intact. In line with this conclusion, the two peaks of the intermediate species are closer to the product signal than those of 2HTPP,

(57) Gassman, P. G.; Ghosh, A.; Almlöf, J. *J. Am. Chem. Soc.* **1992**, *114*, 9990.
(58) Ghosh, A.; Fitzgerald, J.; Gassman, P. G.; Almlöf, J. *Inorg. Chem.* **1994**, *33*, 6057.
(59) Goll, J. G.; Moore, K. T.; Ghosh, A.; Therien, M. J. *J. Am. Chem. Soc.* **1996**, *118*, 8344.

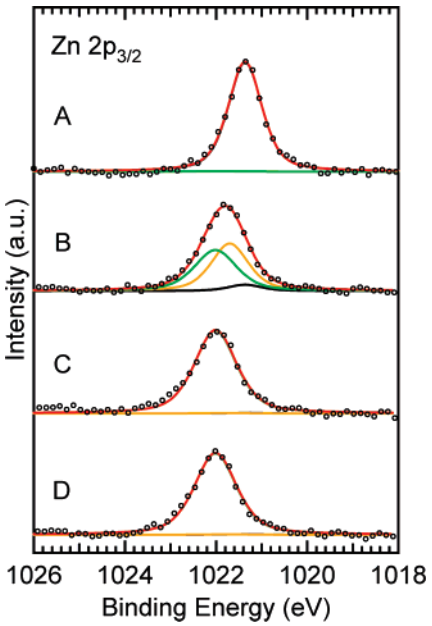

Figure 7. Zn $2p_{3/2}$ spectra of (A) Zn on Ag(111) ($\theta_{Zn} = 0.043$), (B) after deposition of Zn ($\theta_{Zn} = 0.038$) on a monolayer of 2HTPP, and (C) after subsequent heating to 550 K. (D) Zn $2p_{3/2}$ spectrum of a directly deposited monolayer of ZnTPP on Ag(111) for comparison. Line colors: black, Zn^0; green, ZnTPP; orange, intermediate; red, envelope.

which is reasonable because the chemical state of the nitrogen atoms in the initial complex **7** should lie between 2HTPP and ZnTPP. Further evidence for the existence of this species is provided by the Zn $2p_{3/2}$ XPS spectra in Figure 7, in which an intermediate state of Zn is observed. The respective signal component (Figure 7B, orange line) is located at 1021.7 eV, i.e., between the signals of Zn^0 (1021.3 eV, black line) and ZnTPP (1022.2 eV, green line).

Temperature-Programmed Reaction Measurements (TPRMs). The relatively high activation barrier for metalation with Zn (the calculated values are $\Delta E^{\ddagger} = 32.6$ kcal mol^{-1} and $\Delta G^{\ddagger} = 32.8$ kcal mol^{-1} at the B3LYP/6-31G(d) level and $\Delta E^{\ddagger} = 34.8$ kcal mol^{-1} and $\Delta G^{\ddagger} = 35.2$ kcal mol^{-1} at the B3LYP/6-31G(d,p)+LANL2DZ level) made it possible to observe the initial complex **7** in the experiment. To obtain an experimental estimate of this activation energy, we performed a temperature-programmed reaction experiment. A stoichiometric amount of Zn was deposited on a monolayer of 2DTPP (N-deuterated 2HTPP) on Ag(111) at 250 K. Thereafter, the system was heated with a constant rate of 5 K s^{-1} while the release of D_2 (as the expected reaction product) was detected with a mass spectrometer.[60] We found a maximum D_2 production at 510 K (Figure 8). Using Redhead's approximation,[61] we estimated an activation energy of $\Delta E^{\ddagger} = 31$ kcal mol^{-1}, assuming a preexponential factor of 10^{13} s^{-1}. Alternatively, we employed a modified Redhead relation (see the Supporting Information) to estimate a Gibbs activation energy of $\Delta G^{\ddagger} = 32$ kcal mol^{-1} (without making assumptions about the frequency factor). Both values are in excellent agreement with our DFT calculations.

The close agreement between experimental and theoretical values suggests that the influence of the surface on the reactants,

(60) 2DTPP was used because D_2 is easier to detect in a UHV environment, which usually contains H_2 as a residual gas. The differences between the activation energies for 2HTPP (theory) and 2DTPP (experiment) can be neglected at our level of accuracy.
(61) Redhead, P. A. *Vacuum* **1962**, *12*, 203.

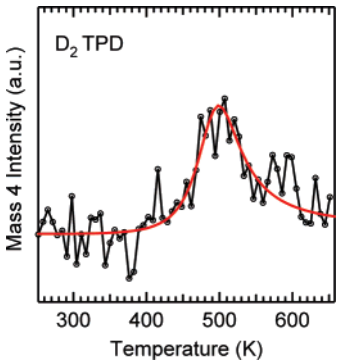

Figure 8. Temperature-programmed reaction curve (detected mass $m/z = 4$) of the reaction between 2DTPP and Zn on a Ag(111) surface. The heating rate was 5.0 K/s. The red line is shown as a guide to the eyes.

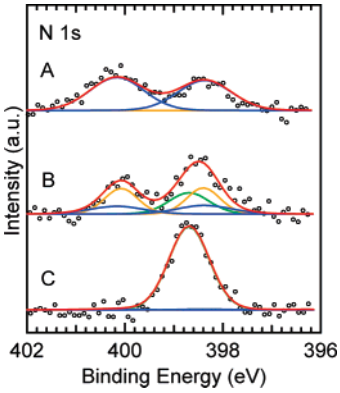

Figure 9. N 1s XPS spectra (A) after deposition of zinc ($\theta_{Zn} = 0.037$) on the Ag(111) surface, followed by deposition of a monolayer of 2HTPP at 115 K, (B) after subsequent warming of the Zn/2HTPP coadsorbate to 300 K, and (C) after heating to 550 K. Line colors: blue, 2HTPP; green, ZnTPP; orange, intermediate; red, envelope.

which was neglected in the DFT calculations, is small. This is not surprising, because, as will be explained below, a substantial influence of the surface on the energetics and kinetics of the reaction is only expected for the first reaction step, in which the initial complex **7** is formed. In the TPR experiment, however, we determine the activation energy of the rate-limiting step, which is the hydrogen transfer from a pyrrolic nitrogen atom to the Zn atom, i.e., an isomerization reaction of the complex in which formally no bond to the surface is formed or broken. In our calculation, we assumed that the metal atom is initially in the gas phase. Accordingly, we find no barrier for the formation of the initial complex. In reality, however, the metal atom may adsorb first on the surface and then diffuse to the reaction site, where it is eventually coordinated. In this case, formation of the initial complex includes cleavage of the chemisorptive bond between the Zn atom and the surface, a process that will certainly result in an activation barrier. Evidence for such a participation of the surface and the existence of this mechanism is provided by our recent study in which Zn was deposited on the Ag surface *prior* to the deposition of the porphyrin.[15] This procedure led to the same result as the reverse order of deposition.

If the formation of the initial complex is indeed activated, as these considerations suggest, then it should be possible to suppress this reaction by sufficiently lowering the temperature. The results of the corresponding low-temperature experiment are shown in Figure 9. Figure 9A shows the N 1s XPS spectrum taken after deposition of zinc ($\theta_{Zn} = 0.037$) on the Ag(111)

surface, followed by deposition of a monolayer of 2HTPP at 115 K. This spectrum is identical to that of a 2HTPP monolayer on the clean Ag(111) surface and thus indicates that no formation of the initial complex occurred. Warming the sample to 300 K, however, clearly induced partial reaction to the initial complex, as revealed by Figure 9B. Heating to 550 K eventually completed the reaction to ZnTPP (Figure 9C). We note that the rate of formation of the initial complex is not necessarily controlled by the insertion of the metal atom into the porphyrin, as was assumed above, but may alternatively be controlled by the diffusion rate of the metal atoms on the surface.

The preceding considerations suggest that the influence of the surface on the kinetics and energetics of the reaction is mainly restricted to the first reaction step, the formation of the initial complex. The further reaction steps should be less affected by the surface, because they are isomerization or decomposition reactions in which no bonds to the surface are formed or cleaved. For further verification of this assumption, calculations that include the surface are under way.

Summary and Conclusions

We have demonstrated that the direct metalation of porphyrins with bare transition-metal atoms proceeds via an initial complex which has a structure similar to that of the SAT complex proposed for reaction of porphyrins with metal ions in solution. In contrast to the situation in solution, the reaction here is a redox process that results in a release of H_2. The rate of this reaction is controlled by the transfer of a pyrrolic N-bound hydrogen atom to the metal center of the initial complex. The activation energy of this rate-limiting step varies for the different metal atoms. For metalation with zinc, we found an activation energy of 31 kcal mol^{-1} in the experiment and 32.6 kcal mol^{-1} with DFT. The overall reactions of Fe, Co, and Ni are very much faster and can be described as potential two-state reactivity processes, whereas those with Cu and Zn proceed on a single potential energy surface.

Acknowledgment. This work was supported by the Deutsche Forschungsgemeinschaft through SFB 583, "Redox-Active Metal Complexes; Control of Reactivity via Molecular Architectures", by a grant of computer time on the Höchstleistungsrechner in Bayern II (HLRB II), and by the award of an Alexander-von-Humboldt Fellowship to T.E.S.

Supporting Information Available: Modified Redhead equation, energy profiles for Ni and Cu atom insertion into 2HP, complete ref 48, and the Gaussian Archive entries and absolute energies for all computed species. This material is available free of charge via the Internet at http://pubs.acs.org.

JA072360T